Accepted Manuscript

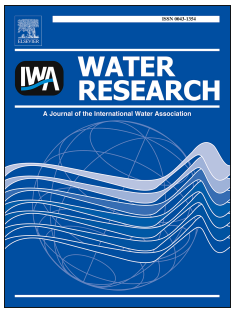

The importance of reactive oxygen species on the aqueous phototransformation of sulfonamide antibiotics: Kinetics, pathways, and comparisons with direct photolysis

Linke Ge, Peng Zhang, Crispin Halsall, Yanying Li, Chang-Er Chen, Jun Li, Helin Sun, Ziwei Yao

PII: S0043-1354(18)30930-8

DOI: https://doi.org/10.1016/j.watres.2018.11.009

Reference: WR 14216

To appear in: *Water Research*

Received Date: 4 July 2018

Revised Date: 2 October 2018

Accepted Date: 4 November 2018

Please cite this article as: Ge, L., Zhang, P., Halsall, C., Li, Y., Chen, C.-E., Li, J., Sun, H., Yao, Z., The importance of reactive oxygen species on the aqueous phototransformation of sulfonamide antibiotics: Kinetics, pathways, and comparisons with direct photolysis, *Water Research*, https://doi.org/10.1016/j.watres.2018.11.009.

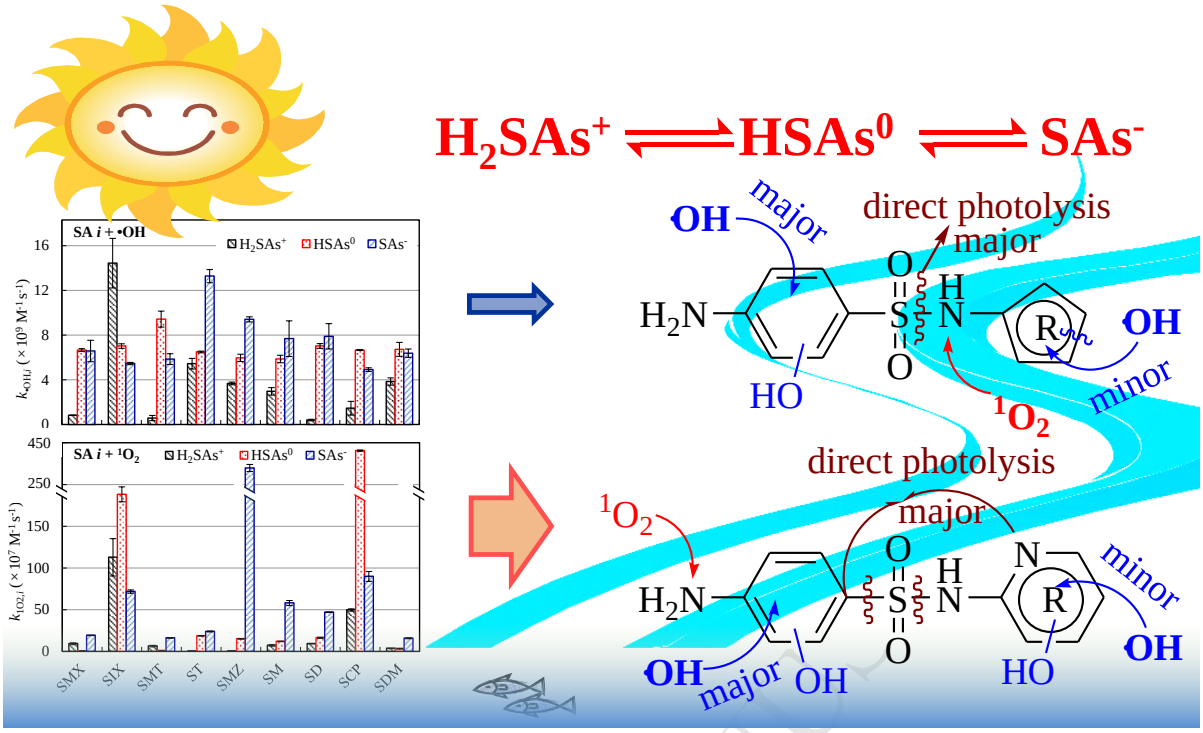

Photooxidation of dissociated sulfonamides (SAs)

The importance of reactive oxygen species on the aqueous phototransformation of sulfonamide antibiotics: Kinetics, pathways, and comparisons with direct photolysis

Linke Ge[a,b], Peng Zhang[a,b], Crispin Halsall[b,*], Yanying Li[b], Chang-Er Chen[c], Jun Li[a], Helin Sun[a], Ziwei Yao[a]

[a] Key Laboratory for Ecological Environment in Coastal Areas (SOA), National Marine Environmental Monitoring Center, Dalian 116023, P. R. China

[b] Lancaster Environment Centre, Lancaster University, Lancaster LA1 4YQ, United Kingdom

[c] Environmental Research Institute, MOE Key Laboratory of Environmental Theoretical Chemistry, South China Normal University, Guangzhou 510006, P. R. China

ABSTRACT

Sulfonamide antibiotics (SAs) are increasingly detected as aquatic contaminants and exist as different dissociated species depending on the pH of the water. Their removal in sunlit surface waters is governed by photochemical transformation. Here we report a detailed examination of the hydroxyl radical (•OH) and singlet oxygen ($^1O_2$) mediated photooxidation of nine SAs: sulfamethoxazole, sulfisoxazole, sulfamethizole, sulfathiazole, sulfamethazine, sulfamerazine, sulfadiazine, sulfachloropyridazine and sulfadimethoxine. Both •OH and $^1O_2$ oxidation kinetics varied depending on the dominant protonated states of the SA in question (H_2SAs^+, $HSAs^0$ and SAs^-) as a function of pH. Based on competition kinetic experiments and matrix deconvolution calculations, $HSAs^0$ or SAs^- (pH ~5–8) were observed to be more highly reactive towards •OH, while SAs^- (pH ~8) react the fastest with $^1O_2$ for most of the SAs tested. Using the empirically derived rates of reaction for the speciated forms at different pHs,

* Corresponding author. Tel./fax: +44 (0)1524 594330.

E-mail address: c.halsall@lancaster.ac.uk (C. Halsall).

the environmental half-lives were determined using typical $^1O_2$ and •OH concentrations observed in the environment. This approach suggests that photochemical $^1O_2$ oxidation contributes more than •OH oxidation and direct photolysis to the overall phototransformation of SAs in sunlit waters. Based on the identification of key photointermediates using tandem mass spectrometry, $^1O_2$ oxidation generally occurred at the amino moiety on the molecule, whereas •OH reaction experienced multi-site hydroxylation. Both these reactions preserve the basic parent structure of the compounds and raise concerns that the routes of phototransformation give rise to intermediates with similar antimicrobial potency as the parent SAs. We therefore recommend that these phototransformation pathways are included in risk assessments concerning the presence and fate of SAs in waste and surface waters.

Keywords: Sulfonamides; dissociated forms; photodegradation; oxidation kinetics; transformation products

1. Introduction

The occurrence, transformation and risks of antibiotics in aquatic systems are well-acknowledged environmental issues and have raised particular concerns (Baena-Nogueras et al., 2017; Luo et al., 2011). Sulfonamides (SAs) are a large class of antibiotics that are widely used in human treatments, animal husbandry and aquaculture (Managaki et al., 2007). Due to their incomplete elimination by metabolism (Campagnolo et al., 2002) and wastewater treatment (Chen et al., 2013), SAs enter the environment continually and are regularly detected as aqueous micropollutants. Their presence in surface waters has been reported in many countries including the United States (Kolpin et al., 2002), Europe (Loos et al., 2009), Vietnam (Managaki et al., 2007) and China (Luo et al., 2011). Concentrations in surface waters can vary quite widely, with mean concentrations observed to range from 0.1 to 150.8 ng L^{-1} in the coastal waters of China through a variety of recent

monitoring studies (see Fig. S1 and associated references). There is evidence of ecotoxicological effects of SAs on freshwater biota, with SAs also promoting bacterial resistance (Białk-Bielińska et al., 2017; Białk-Bielińska et al., 2011; Zhang et al., 2015). Interestingly, exposure to sunlight appears to enhance the toxicities of SAs towards several aquatic organisms, such as *D. magna* (Jung et al., 2008; Trovó et al., 2009b), and *Vibrio fischeri* (Xu et al., 2014) and this reflects the toxicity exhibited by other photo-transformed antibiotics, such as fluoroquinolones (Ge et al., 2010; Ge et al., 2018).

SAs may undergo different transformation processes including photodegradation and biodegradation. However, in sunlit surface waters, photodegradation has been identified as the major transformation pathway (Carstens et al., 2013). Specifically, SAs can undergo direct photodegradation as well as sensitized indirect photoprocesses such as oxidation reactions with hydroxyl radicals (•OH), singlet oxygen ($^1O_2$), and other reactive oxygen species (ROS) (Boreen et al., 2004, 2005; Li et al., 2018). In sunlit surface waters, •OH and $^1O_2$ are ubiquitous in waters and serve as the most important transient photooxidants leading to the oxidative degradation of aqueous organic micropollutants (Cooper et al., 1989; Vione et al., 2014; Zhang et al., 2014). They are generated from sunlight-induced reactions involving common water constituents, such as dissolved organic matter (DOM), nitrate ions, and Fe(III). Furthermore, the environmental photochemical processes of SAs can also be affected by the presence of other water constituents such as halide ions, HCO_3^- and Cu^{2+} ions (Guerard et al., 2009; Li et al., 2018; Li et al., 2016; Niu et al., 2013a). As the molecular structures of SAs contain two ionizable groups (i.e., $-NH_2$ and $-NH-$), their various dissociated forms are expected to influence their photochemical behavior (Boreen et al., 2004; Wei et al., 2013), although the behavior of the various dissociated forms is not well understood.

Previous studies have demonstrated separate phototransformation kinetics of different dissociated species for specific compounds in various classes of antibiotics, such as

tetracyclines (Niu et al., 2013b; Werner et al., 2006), fluoroquinolones (Ge et al., 2015; Wei et al., 2013), and SAs (Boreen et al., 2004, 2005; Willach et al., 2018), although for SAs direct photodegradation rather than ROS photooxidation has been the focus to date. For direct photodegradation, the anionic, neutral and cationic species of SAs have different quantum yields (Φ) and rate constants (k), and the most photoreactive component varies depending on the SA under investigation (Bonvin et al., 2013; Boreen et al., 2004, 2005; Niu et al., 2013a; Xu et al., 2014). Without considering the protonation state, SAs react with •OH at a mean rate (k) of 5.3×10^{9} M^{-1} s^{-1}, and their $^{1}O_2$ oxidation k ranges over 4 orders of magnitude (10^{4}–10^{8}) (Boreen et al., 2004, 2005). The different protonation states are expected to react with ROS at different reactivities. However, the ROS photooxidation kinetics of the different dissociation species has received little attention in the literature. Furthermore, to apportion the relative contributions of the photooxidation to the fate of SAs, the corresponding environmental half-lives in surface waters need to be assessed based on the distribution of the speciated forms and the ambient water conditions.

A thorough understanding of the transformation routes via ROS photooxidation of SAs is important for the overall assessment of their aquatic fate and to understand the relative importance of this phototransfromation pathway compared to direct photodegradation. To date, only several intermediates have been identified for selected SAs for the oxidation reaction with •OH in advanced oxidation processes (Batista et al., 2014; Du et al., 2018; Hu et al., 2007; Trovó et al., 2009a). The •OH can induce multihydroxylation of the aniline moiety, and cleavage of heterocyclic rings (Batista et al., 2014; Hu et al., 2007; Shah and Hao, 2017). As for $^{1}O_2$ oxidation, some relevant mechanisms have been proposed. For example, a [2+2] cycloaddition of $^{1}O_2$ on isoxazole rings was speculated for SAs containing five-membered heterocyclic groups (Boreen et al., 2004). Furthermore, $^{1}O_2$ tends to oxidate electron-rich compounds, such as anilines, dialkyl sulfides, pyrroles, and phenolate anions (Mill, 1999).

These previous studies provide a useful rationale to further investigate ROS photooxidation of SAs in an environmental context.

The purpose of this study was to investigate the ROS (i.e., •OH and $^1O_2$) oxidation kinetics of SAs and compare the oxidation products and kinetics with those formed from direct photodegradation. The nine SAs selected in the study are widely used and commonly reported in aquatic environments (Chen et al., 2013; Kolpin et al., 2002; Luo et al., 2011; Managaki et al., 2007). Importantly, the oxidation kinetics and reactivities were examined for the various dissociated forms which, in turn, are dependent on the ambient pH. ROS-induced transformation pathways are currently under-represented in the literature and yet may account for a signficant proportion of phototransformation of SAs in surface waters. This has important implications for how we assess their fate and undertake environmental risk assessments for this group of chemicals.

2. Materials and methods

2.1. Reagents and materials

Four SAs containing the five-membered heterocyclic groups and five SAs containing the six-membered heterocyclic groups were selected as model compounds for the study (Fig. 1), including sulfamethoxazole (SMX), sulfisoxazole (SIX), sulfamethizole (SMT), sulfathiazole (ST), sulfamethazine (SMZ), sulfamerazine (SM), sulfadiazine (SD), sulfachloropyridazine (SCP), and sulfadimethoxine (SDM). As described in Table S1, the nine SAs were purchased from different suppliers. All the compounds, as received, were at least 98% purity. Furfuryl alcohol (FFA, 98%) and perinaphthenone (97%) were obtained from J&K Technology Co., Ltd. and Sigma-Aldrich, respectively. Hydrogen peroxide (H_2O_2, 30%) was purchased from Acros Organics. Methanol, trifluoroacetic acid and acetophenone (AP) were of HPLC grade, and other reagents such as phosphates were of guaranteed grade and used as received. All

solutions were prepared in ultrapure water obtained from a Millipore-Milli Q system.

Fig. 1. Chemical structures and the different protonation states of sulfonamide antibiotics (SAs), where H_2SAs^+, $HSAs^0$, and SAs^- represent the cationic form, the neutral form, and the anionic form, respectively.

2.2. Photochemical experiments

A merry-go-round reactor with quartz tubes (50 mL volume and 20 mm diameter) containing reaction solutions was used to perform photochemical experiments under irradiation of a water-refrigerated 500W high-pressure mercury lamp. The light intensities at the solutions were 1.95 mW cm^{-2} at 365 nm and 1.83 mW cm^{-2} at 420 nm, measured by a UV spectral irradiometer (Photoelectric Instrument Factory of Beijing Normal University). The experimental setup and spectral irradiance are illustrated in Figs. S2 and S3, respectively. Competition kinetics were employed to determine the bimolecular rate constants k_{ROS} (i.e., $k_{\bullet OH}$ and k_{1O2}) for the reactions between SAs and ·OH according to Eq. (1):

$$k_{ROS}^{S} = \frac{\ln([S_t]/[S_0])}{\ln([R_t]/[R_0])} k_{ROS}^{R} \quad (1)$$

where S is the substrate SAs, R is a reference compound, and the square brackets [] represent the concentrations. The method has been used successfully to examine the •OH/$^1O_2$ reactivifties of pharmaceuticals and other environmental organic contaminants (Boreen et al., 2004; Edhlund et al., 2006; Wei et al., 2015; Xie et al., 2013).

The initial concentration of individual SAs was set at 10 μM. Hydroxyl radicals (•OH) were generated through the addition of H_2O_2 (100 mM) with a 340 nm cut-off filter surrounding the Hg-lamp light source. Acetophenone (10 μM) was spiked into the reaction solution as the reference compound with $k_{\bullet OH} = 5.9 \times 10^9$ M^{-1} s^{-1} (Edhlund et al., 2006). For the $^1O_2$ reaction experiments 380 nm cut-off filters were used for the light source, with

perinaphthenone (20 μM) and furfuryl alcohol (20 μM) as the photosensitizer and reference compound (k_{1O2} = 1.2 × 10^8 M^{-1} s^{-1}), respectively. Perinaphthenone is often used to photogenerate $^1O_2$ with a quantum yield close to unity (Boreen et al., 2008; Han et al., 2008; Latch et al., 2003; Oliveros et al., 1991; Schmidt et al., 1994). The $^1O_2$ reaction solutions were pre-aerated to be saturated with dissolved oxygen. The pH of the reaction solutions (pH = 2, 5 and 8) was adjusted to the desired value using phosphate buffers. All the competition kinetic experiments with controls were conducted in triplicate.

2.3. Matrix deconvolution calculation

The ROS oxidation rate constants ($k_{ROS,i}$) for SA protonation states (i) were calculated using matrix deconvolution methods, based on previous studies (Boreen et al., 2004, 2005; Werner et al., 2006) and used successfully by our group in a previous study on ionisable fluoroquinolones (Ge et al., 2018). For each SA, the individual $k_{\bullet OH,i}$ or $k_{1O2,i}$ of the fully protonated (H_2SAs^+), neutral ($HSAs^0$), and anionic forms (SAs^-) were fitted according to the following Matrix (1):

$$\begin{array}{c} \text{pH 2} \\ \\ \text{pH 8} \end{array} \begin{pmatrix} \delta_{H_2SAs^+}, & \delta_{HSAs^0}, & \delta_{SAs^-} \\ \text{M} & & \text{M} \\ \text{M} & & \text{M} \end{pmatrix} \begin{pmatrix} k_{ROS,H_2SAs^+} \\ k_{ROS,HSAs^0} \\ k_{ROS,SAs^-} \end{pmatrix} = \begin{pmatrix} k_{ROS} \\ \text{M} \\ \text{M} \end{pmatrix}_{\text{pH 8}}^{\text{pH 2}} \quad (1)$$

where δ_i represents the fraction of each dissociated form and the values are referred to in Fig. S4, k_{ROS} is $k_{\bullet OH}$ or k_{1O2} of SAs at different pH, and $k_{ROS,H2SAs+}$ − $k_{ROS,SAs-}$ are the $k_{\bullet OH,i}$ or $k_{1O2,i}$ of the three SA forms to be fitted.

2.4. Analytical Determination

A Waters UPLC with PDA detector, fitted with a BEH C18 column, was employed for the separation and quantification of SAs, acetophenone and furfuryl alcohol in the irradiated samples, which were collected from the reactor and spiked with methanol (•OH quencher) or NaN_3 ($^1O_2$ quencher). To identify intermediates, irradiated solutions (2 L for each sample)

was purified by solid phase extraction and then analyzed by an Agilent HPLC coupled to a triple quadrupole mass spectrometer operating in both positive and negative modes. The analytical details are provided in the Supplementary material.

3. Results and discussion

3.1. ROS oxidation kinetics under different pH

In the control experiments, the losses of SAs and reference compounds either under dark or in the absence of the ROS photosensitizer were <2%. Thus, degradation by direct photolytic, thermal and hydrolytic processes was considered negligible during the duration of the photochemical experiments (2 hrs). However, when exposed to light irradiation in the competition kinetic experiments, the SAs disappeared quickly, indicating that the SAs were photooxidised efficiently by ROS. The oxidative degradation curve of SMZ as an example is provided in Fig. S5. The values for the bimolecular reaction rate constants of the nine SAs with •OH ($k_{\bullet OH}$) and $^1O_2$ (k_{1O2}) in pure water are listed in Tables S2 and S3. The $k_{\bullet OH}$ ranged from $(5.00 \pm 0.77) \times 10^9$ M^{-1} s^{-1} for SM to $(9.16 \pm 1.66) \times 10^9$ M^{-1} s^{-1} for SMT, while the k_{1O2} ranged from $(2.31 \pm 0.06) \times 10^7$ M^{-1} s^{-1} for SMX to $(1.34 \pm 0.15) \times 10^9$ M^{-1} s^{-1} for SCP. The $k_{\bullet OH}$ values were larger than k_{1O2}, indictive of the higher reactivity of •OH with the various SA compounds. However, considering that the steady-state concentrations of $^1O_2$ can be three-orders of magnitude higher than that of •OH (Cooper et al., 1989; Mill, 1999), $^1O_2$ may be more important than •OH in the attenuation of SAs in sunlit waters.

In comparison with other antibiotics, the $k_{\bullet OH}$ values of SAs fall in the same order of magnitude as the fluoroquinolones (Ge et al., 2015; Santoke et al., 2009), tetracyclines (Jeong et al., 2010), and nitrofurans (Edhlund et al., 2006). However, the k_{1O2} of SAs are 1 – 3 orders of magnitude greater than those observed for the other antibiotics (Castillo et al., 2007; Edhlund et al., 2006; Wei et al., 2015). This notable difference of k_{1O2} among antibiotics can

be attributed to the higher selectivity of $^1O_2$ than that of •OH to oxidize organic chemicals (Keen and Linden, 2013; Larson and Weber, 1996; Mill, 1999; Yao et al., 2013). •OH can oxidize almost all classes of organic chemicals (Keen and Linden, 2013; Li et al., 2014; Mill, 1999), whereas $^1O_2$ is more sensitive to electron-rich chemicals, such as sulfides and phenols (Larson and Weber, 1996; Mill, 1999).

Since aqueous SAs can undergo two acid-base dissociation processes (Fig. S4), the ROS oxidation reactivity of each SA is expected to depend on its speciation at a given pH value. To quantify the reactivity of each protonation state towards •OH and $^1O_2$, the $k_{\bullet OH}$ and k_{1O2} were determined for three different pHs. The results are illustrated in Fig. 2, and the corresponding values are provided in Tables S2 and S3. It is found that both $k_{\bullet OH}$ and k_{1O2} are dependent on pH ($p < 0.05$), with generally higher values of $k_{\bullet OH}$ at pH 5 and pH 8 than at pH 2, although SIX was the exception to this, displaying the fastest reactivity at pH 2. Similarly, the reactivity of $^1O_2$ oxidation was fastest for seven of the SAs at pH 8, while only two SAs, SIX and SCP, had the fastest kinetics at pH 2 and pH 5, respectively. The higher reactivity of SIX at pH 2 suggests that the reactive site might be the dimethylisoxazole moiety towards •OH and $^1O_2$ at the lower pH. For SMX with its monomethylisoxazole moiety, dimethylation of the isoxazole ring significantly increases the electron density of this ring (Dogan et al., 1990), making SIX more susceptible to ROS attack, particularly to $^1O_2$ oxidation (Fig. 2).

The effect of pH on the $^1O_2$ oxidation kinetics was more significant than the reaction with •OH. For example, the k_{1O2} values showed a 1.3- to 11.2-fold variation (mean = 4.5) over the pH range, while $k_{\bullet OH}$ showed a 1.5- to 4.3-fold variation (mean = 2.2). The $k_{\bullet OH}$ and k_{1O2} values reported here compare favourably to an earlier study examining the photochemical fate of SAs (Boreen et al., 2004, 2005). In this case, k_{1O2} was only measured at pH 10.2 (carbonate-buffered solution) and $k_{\bullet OH}$ at pH 3 (Fenton system), with k_{1O2} for SMT reported as $(5.5 \pm 0.4) \times 10^7$ M^{-1} s^{-1} and $k_{\bullet OH}$ as $(6.6 \pm 0.2) \times 10^9$ M^{-1} s^{-1} (Boreen et al., 2004, 2005). For

other chemicals, the pH effect resulting in different protonation states and their corresponding ROS reactivities has been reported for fluoroquinolone antibiotics (Ge et al., 2015; Wei et al., 2013) and hydroxylated polybrominated diphenyl ethers (Xie et al., 2013).

Fig. 2. ROS oxidation rate constants ($k_{\bullet OH}$ and k_{1O2}) of 9 sulfonamide antibiotics (SAs) under different pH conditions

3.2. ROS reactivities of different dissociated species

As shown in Fig. 3, ROS reactivities of SA dissociated species (*i*) are represented with the calculated bimolecular reaction rate constants ($k_{\bullet OH,i}$ and $k_{1O2,i}$). Their corresponding values are listed in Tables S4 and S5. Each SA showed variable ROS reactivities for the different dissociated forms, H_2SAs^+ to SAs^-. With the exception of SIX，the other eight SAs in their neutral ($HSAs^0$) or anionic (SAs^-) forms were more highly reactive towards •OH whereas most of the SAs (other than SIX and SCP) showed the fastest reaction with $^1O_2$ in their anionic form (SAs^-). Compared with •OH oxidation, the $^1O_2$ reaction activities varied by several orders of magnitude across the various speciated forms of the different SAs (e.g. H_2SAs^+ to SAs^-). The proportion of each form is dependent on the pH (e.g. 2 to 8). Increasing pH enhances the deprotonation and electron density of the reactive aniline moiety, which in turn increases the electron donating ability and decreases the steric hindrance, thus making the aniline more vulnerable toward ROS oxidant/radical attack (Dodd et al., 2006; Jiao et al., 2008; Wei et al., 2013). For example, the aniline moiety in SMX makes this compound more susceptible to electrophilic O_3 attack particularly following deprotonation experienced at higher pHs (Dodd et al., 2006).

For emerging micropollutants including antibiotics, a database of $k_{ROS,i}$ values was constructed to describe the reactivities of their different protonated states towards •OH and $^1O_2$ (Table S6). This table includes the $k_{\bullet OH,i}$ and $k_{1O2,i}$ for SAs from this study, as well as

values for a selection of ionisable antibiotics, flame retardants and other relevant chemicals of environmental concern. Similar to the SAs investigated here, anionic forms of all other chemicals react faster with $^1O_2$ than neutral or cationic forms. Tetracyclines in their neutral or anionic forms were more highly reactive towards •OH. However, fluoroquinolones in their neutral form showed higher reactivities of •OH than in their protonated/cationic and anionic forms (Ge et al., 2018; Ge et al., 2015), while anionic HO-PBDEs were oxidised faster by •OH than the neutral forms (Xie et al., 2013). These ROS reactive patterns, coupled to the dominant speciated form of the chemical, are of importance for the fate assessment of the ionisable pollutants that usually coexist with •OH and $^1O_2$ in surface waters.

Fig. 3. Bimolecular rate constants ($k_{\bullet OH,i}$ and $k_{1O2,i}$) for the reaction between dissociated SA species (SA *i*) species and ROS

3.3. Photooxidation half-lives in surface waters

In sunlit surface waters, the photoinduced •OH and $^1O_2$ radicals are the most important transient oxidants (Cooper et al., 1989; Vione et al., 2014; Zhang et al., 2014). Their concentrations ([ROS]) range from 10^{-17} to 10^{-15} M and from 10^{-15} to 10^{-12} M, respectively (Cooper et al., 1989; Mill, 1999). Based on ROS reactivities of dissociated SA species, the corresponding environmental half-lives ($t_{1/2,ROS,E}$, i.e., $t_{1/2,\bullet OH,E}$ and $t_{1/2,1O2,E}$) at a specific pH can be calculated according to Eqs. 2 – 3:

$$k_{ROS,E} = [ROS]\sum(\delta_i k_{ROS,i}) \quad (2)$$

$$t_{1/2,ROS,E} = \frac{\ln 2}{k_{ROS,E}} \quad (3)$$

where $k_{ROS,E}$ is the environmental rate constant of SAs towards •OH or $^1O_2$; $k_{ROS,i}$ represents $k_{\bullet OH,i}$ or $k_{1O2,i}$; and δ_i values (i.e. the fraction of each dissociated form) are taken from Fig. S4. The calculation method takes into account the acid-base dissociation of SAs and the

pH-dependent kinetics of ROS oxidation, and is also applicable for the calculation of the $t_{1/2,ROS,E}$ of other dissolved ionizable organic pollutants. Previous studies have tended to assess the $t_{1/2,ROS,E}$ without considering the pH difference between laboratory solutions and surface waters (Boreen et al., 2004, 2005).

As shown in Table 1, the calculated values of $t_{1/2,\bullet OH,E}$ and $t_{1/2,1O2,E}$ for the nine SAs range from 14.62 h to 39.23 h and from 0.06 h to 2.22 h, respectively. To assess the importance of the photooxidation on the fate of SAs, $t_{1/2,ROS,E}$ values were compared with direct photolytic half-lives ($t_{1/2,D,E}$) of SAs in near surface waters (Boreen et al., 2004, 2005). For individual SAs, $t_{1/2,1O2,E}$ are considerably shorter than $t_{1/2,\bullet OH,E}$ and $t_{1/2,D,E}$, indicating that oxidation of SAs towards $^1O_2$ can be a central factor in their environmental phototransformation. Even though •OH is an unselective, highly reactive species, the environmental fate of SAs is likely not controlled by the reaction with •OH, which can be attributed to such low concentrations of •OH in surface waters. However, since the $t_{1/2,\bullet OH,E}$ are comparable to $t_{1/2,D,E}$ in midsummer and less than $t_{1/2,D,E}$ in midwinter, suggesting •OH oxidation is also appreciable compared to direct photolysis. Furthermore, the •OH is expected to be more effective at degrading SAs due to its non-selectivity (Ge et al., 2015; Keen and Linden, 2013; Li et al., 2014; Mill, 1999).

The values in Table 1 represent the minimum expected half-lives, as these were calculated based on the highest ROS levels and continual light irradiation, although the phototransformation may be hindered by light scattering, or limited photic zone depth. Apart from the photooxidation and direct photolysis, SAs may undergo solar photosensitized degradation via ^{3}DOM, which is of significance in most waters (Boreen et al., 2005; Li et al., 2015). In addition, concomitant metal ions can also influence the photochemical behavior of SAs by complexation effects (Shah et al., 2015; Wei et al., 2015). Thus, to better understand the environmental photochemical fate of SAs, further studies are needed to study specific water bodies and examine the effects of non-continuous solar exposure, water depth and other

aqueous constituents that may attenuate or absorb sunlight (Bodrato and Vione, 2014).

Table 1 Expected environmental half-lives ($t_{1/2,E}$, h) for reactions with either •OH or $^1O_2$, and direct photodegradation of sulfonamides (SAs) in sunlit surface waters.

[a] Calculated based on the •OH and $^1O_2$ concentration levels in the euphotic zone of some surface waters, i.e., [•OH] = 1×10^{-15} M and [$^1O_2$] = 1×10^{-12} M (Cooper et al., 1989; Mill, 1999). [b] Corresponding to direct photolytic half-lives of SAs in near surface waters in midsummer and midwinter at 45° latitude (Boreen et al., 2004, 2005). The half-lives were calculated with quantum yields (correcting for lens effect) and noon-averaged tabulated solar intensities (assuming continuous irradiation) (Leifer, 1988).

3.4. ROS oxidation intermediates and pathways

Four SAs, comprising of SIX, ST, SMZ and SCP were selected to investigate their phototransformation byproducts and deduce their main transformation pathways based on the three different reactions including $^1O_2$ and •OH oxidation, as well as direct photolysis. We identified 21 significant intermediates generated from their photooxidation. All details on the identification of these photoproducts are shown in Table S7, including chromatographic retention times, molecular weight (M_w), as well as mass spectral parent and fragment ions, *m*/*z*. The corresponding MS and MS^2 mass spectra in positive ionisation mode are displayed in Fig. S6. Referring to the Nitrogen rule and the analytical approaches in previous studies (Baena-Nogueras et al., 2017; Sági et al., 2015), chemical structures were proposed and tentative phototransformation pathways for the four SAs are presented in Fig. 4.

There are three types of transformation pathways (Paths 1–3), corresponding to the three different reactions of each SA (Fig. 4). Among the $^1O_2$ oxidation reactions (Path 1), complexes occur through –R group addition at the sulfonyl-N (N^1) site for SAs containing five-membered heterocyclic substituents, whereas SAs with six-membered heterocyclic groups experience an oxidation at the amino-N (N^{11}) site. As for transformation products with

molecular weight of 352 (TP352a/TP352b), the –R groups involve one nitrogen atom. TP292 of SMZ generated from the addition of $^1O_2$ to amino-N, and other moieties of SMZ were not transformed due to the detection of main fragment ions with *m*/*z* = 186 and 124 (Fig. S6) (Sági et al., 2015). A $^1O_2$ oxidative product similar to TP292 was also reported for sulfapyridine (Xu et al., 2014). Besides, Li et al., (2015) revealed that N^1 and N^{11} are also the reaction sites for the reactions of SD with excited triplet state of DOM proxies. Boreen et al., (2004) speculated that the electron-rich alkene in the isoxazole ring would be susceptible to singlet oxygenation for SIX. However, the corresponding products were not detected.

In Path 2 (Fig. 4), the reaction of •OH radicals to each SA generated diverse hydroxylated products, which involved multiple photooxidation pathways: phenyl hydroxylation, heterocyclic hydroxylation and cleavage, as well as amino-N oxidation and removal. These multi-pathways can be prioritized based on the by-product abundance in the total ion chromatograms. TP283, TP271, TP294a and TP300b showed optimal responses respectively for the four SAs, suggesting that phenyl hydroxylation is the most prevalent pathway. This can be attributed to the electron-rich aniline moiety that favors the hydroxylation, which in turn promotes further •OH addition, i.e., multihydroxylation (Batista et al., 2014; Shah and Hao, 2017). In comparison, hydroxylated heterocyclic reactions can be considered as minor or secondary pathways, which generated products with small responses (TP255, TP289, TP294b and TP310). Hu et al. also detected similar hydroxy intermediates for UVA-TiO_2 photocatalyzed SMX degradation (Hu et al., 2007). Though some intermediates were not identified, •OH could induce the cleavage of C−S and N−S bonds, thereby generating low-molecular-mass photo-byproducts, and leading ultimately to the full mineralisation of these pollutants into CO_2, H_2O and other inorganic compounds (Batista et al., 2014; Hu et al., 2007).

In Path 3 (Fig. 4), direct photodegradation occurs through a cleavage at various positions

for SAs containing five-membered heterocyclic groups, with sulfanilic acid (TP173) being observed as a common byproduct (Boreen et al., 2004). However, SAs containing six-membered heterocyclic substituents are primarily transformed to desulfonation products (TP214 and TP220) with the loss of SO_2 (Boreen et al., 2005). The SO_2 extrusion can be attributed to aromatic nucleophilic substitution of an aniline radical cation and subsequent Smiles rearrangement (Tentscher et al., 2013). Except for the primary pathways, more direct photolytic intermediates and processes have also been reported for several SAs, including ST (Niu et al., 2017), SMX (Baena-Nogueras et al., 2017), SMZ and sulfapyridine (García-Galán et al., 2012), as well as their human metabolites (Bonvin et al., 2013; García-Galán et al., 2012).

Finally, the knowledge aquired through deducing the reaction pathways provides fundamental insights into the photochemical fate of SAs. In turn this will allow the evaluation of the phototransformation of SAs during wastewater treatment and the wider aquatic environment as part of a detailed risk assessment process. The distinct pathways of SAs during reaction with •OH would support the understanding of relevant mechanisms in advanced oxidation processes (where •OH is dominant), such as UV/Fenton (Trovó et al., 2009a), TiO_2 photocatalysis (Yang et al., 2010) and Fe^0/bisulfite/O_2 systerms (Du et al., 2018). Interestingly, compared to direct photolysis that generally leads to photoproducts of low antimicrobial potency (Niu et al., 2017), ROS photooxidation of the SAs does not initially destroy the core backbone structure of the molecule, indicating that the antibacterial activity may persist in these initial intermediates. Therefore, further studies are required to screen or examine the antimicrobial activities of ROS oxidation products (see Ge et al., 2018).

Fig. 4. Proposed phototransformation pathways of four sulfonamide antibiotics, sulfisoxazole (SIX), sulfathiazole (ST), sulfamethazine (SMZ), sulfachloropyridazine (SCP). The transformation products are labeled "TP*n*", with *n* standing for the molecular weight. Pathways of direct photolysis are referred to the

previous study (Boreen et al., 2004, 2005).

4. Conclusion

This study provides a detailed examination of the aqueous photooxidation of nine widely detected sulfonamide antibiotics (SAs), and shows that photochemical behavior can be greatly influenced by the prevailing major dissociated forms of the SAs in question. The oxidation kinetics of SAs towards •OH and $^1O_2$ were found to be dependent on pH, which was attributable to the disparate reactivities of individual SA protonated states. Among the three dissociated forms, $HSAs^0$ or SAs^- were more highly reactive towards •OH in most cases, while SAs^- reacted the fastest with $^1O_2$ for the majority of the SAs. The expected environmental half-lives in sunlit surface waters suggested that $^1O_2$ oxidation can be a central factor in determining the fate of SAs (especially in waters with a pH > 7), with •OH oxidation also contributing appreciably to phototransformation relative to direct photolysis. Moreover, the three reactions involved different primary transformation pathways and the creation of multiple intermediates. Unlike direct photodegradation, $^1O_2$ oxidation preferred to occur at the sites of the amino moiety, whereas •OH reaction experienced multi-site oxidation with phenyl hydroxylation prevailing as the major pathway. Many of these primary photo byproducts still retained the core chemical structure of the parent SA, which suggests that these compounds may present similar ecotoxicity and antibacterial activity as the parent chemicals.

Acknowledgements

This study was supported by the National Natural Science Foundation of China (21577029 and 41476084), and China Scholarship Council (CSC) Scholarship (201704180014 and 201704180009). The authors are grateful to two anonymous reviewers for their useful insight and additional information regarding the formation of phototransformation by-products.

Appendix A. Supplementary data

Supplementary data to this article can be found online at http://dx.doi.org/10.1016/j.watres.2018.08.026.

References

Baena-Nogueras, R.M., González-Mazo, E., Lara-Martín, P.A., 2017. Photolysis of antibiotics under simulated sunlight irradiation: Identification of photoproducts by high-resolution mass spectrometry. Environ. Sci. Technol. 51, 3148–3156.

Batista, A.P.S., Pires, F.C.C., Teixeira, A.C.S., 2014. The role of reactive oxygen species in sulfamethazine degradation using UV-based technologies and products identification. J. Photochem. Photobiol. A 290, 77–85.

Białk-Bielińska, A., Caban, M., Pieczyńska, A., Stepnowski, P., Stolte, S., 2017. Mixture toxicity of six sulfonamides and their two transformation products to green algae Scenedesmus vacuolatus and duckweed Lemna minor. Chemosphere. 173, 542–550.

Białk-Bielińska, A., Stolte, S., Arning, J., Uebers, U., Böschen, A., Stepnowski, P., Matzke, M., 2011. Ecotoxicity evaluation of selected sulfonamides. Chemosphere. 85, 928–933.

Bodrato, M., Vione, D., 2014. APEX (Aqueous Photochemistry of Environmentally occurring Xenobiotics): a free software tool to predict the kinetics of photochemical processes in surface waters. Environ. Sci. − Proc. Imp. 16, 732–740.

Bonvin, F., Omlin, J., Rutler, R., Schweizer, W.B., Alaimo, P.J., Strathmann, T.J., McNeill, K., Kohn, T., 2013. Direct photolysis of human metabolites of the antibiotic sulfamethoxazole: Evidence for abiotic back-transformation. Environ. Sci. Technol. 47, 6746–6755.

Boreen, A.L., Arnold, W.A., McNeill, K., 2004. Photochemical fate of sulfa drugs in the aquatic environment: Sulfa drugs containing five-membered heterocyclic groups. Environ. Sci. Technol. 38, 3933–3940.

Boreen, A.L., Arnold, W.A., McNeill, K., 2005. Triplet-sensitized photodegradation of sulfa drugs containing six-membered heterocyclic groups: Identification of an SO_2 extrusion photoproduct. Environ. Sci. Technol. 39, 3630–3638.

Boreen, A.L., Edhlund, B.L., Cotner, J.B., McNeill, K., 2008. Indirect photodegradation of dissolved free amino acids: The contribution of singlet oxygen and the differential reactivity of DOM from various sources. Environ. Sci. Technol. 42, 5492–5498.

Campagnolo, E.R., Johnson, K.R., Karpati, A., Rubin, C.S., Kolpin, D.W., Meyer, M.T.,

Esteban, J.E., Currier, R.W., Smith, K., Thu, K.M., McGeehin, M., 2002. Antimicrobial residues in animal waste and water resources proximal to animal feeding operations. Sci. Total Environ. 299, 89–95.

Carstens, K.L., Gross, A.D., Moorman, T.B., Coats, J.R., 2013. Sorption and photodegradation processes govern distribution and fate of sulfamethazine in freshwater-sediment microcosms. Environ. Sci. Technol. 47, 10877–10883.

Castillo, C., Criado, S., Díaz, M., García, N.A., 2007. Riboflavin as a sensitiser in the photodegradation of tetracyclines. Kinetics, mechanism and microbiological implications. Environ. Pollut. 72, 178–184.

Chen, C.E., Zhang, H., Ying, G.G., Jones, K.C., 2013. Evidence and recommendations to support the use of a novel passive water sampler to quantify antibiotics in wastewaters. Environ. Sci. Technol. 47, 13587–13593.

Cooper, W.J., Zika, R.G., Petasne, R.G., Fischer, A.M., 1989. Sunlight-induced photochemistry of humic substances in natural waters: Major reactive species. In: H, I.,MacCarthy, P. (Eds.), Aquatic Humic Substances, Suffet. American Chemical Society,Washington, DC, pp. 333–362.

Dodd, M.C., Buffle, M.O., Von Gunten, U., 2006. Oxidation of antibacterial molecules by aqueous ozone: Moiety-specific reaction kinetics and application to ozone-based wastewater treatment. Environ. Sci. Technol. 40, 1969–1977.

Dogan, I., Steenken, S., Schulte-Frohlinde, D., Icli, S., 1990. Electron spin resonance and pulse radiolysis studies on the reaction of $OH^{\bullet}$ and $SO_4^{\bullet-}$ with five-membered heterocyclic compounds in aqueous solution. J. Phys. Chem. 94, 1887–1894.

Du, J., Guo, W., Wang, H., Yin, R., Zheng, H., Feng, X., Che, D., Ren, N., 2018. Hydroxyl radical dominated degradation of aquatic sulfamethoxazole by Fe^0/bisulfite/O_2: Kinetics, mechanisms, and pathways. Water Res. 138, 323–332.

Edhlund, B.L., Arnold, W.A., McNeill, K., 2006. Aquatic photochemistry of nitrofuran antibiotics. Environ. Sci. Technol. 40, 5422–5427.

García-Galán, M.J., Díaz-Cruz, M.S., Barceló, D., 2012. Kinetic studies and characterization of photolytic products of sulfamethazine, sulfapyridine and their acetylated metabolites in water under simulated solar irradiation. Water Res. 46, 711–722.

Ge, L.K., Chen, J.W., Wei, X.X., Zhang, S.Y., Qiao, X.L., Cai, X.Y., Xie, Q., 2010. Aquatic photochemistry of fluoroquinolone antibiotics: Kinetics, pathways, and multivariate effects of main water constituents. Environ. Sci. Technol. 44, 2400–2405.

Ge, L.K., Halsall, C., Chen, C.E., Zhang, P., Dong, Q.Q., Yao, Z.W., 2018. Exploring the

aquatic photodegradation of two ionisable fluoroquinolone antibiotics – gatifloxacin and balofloxacin: Degradation kinetics, photobyproducts and risk to the aquatic environment. Sci. Total Environ. 633, 1192–1197.

Ge, L.K., Na, G.S., Zhang, S.Y., Li, K., Zhang, P., Ren, H.L., Yao, Z.W., 2015. New insights into the aquatic photochemistry of fluoroquinolone antibiotics: Direct photodegradation, hydroxyl-radical oxidation, and antibacterial activity changes. Sci. Total Environ. 527–528C, 12–17.

Guerard, J.J., Chin, Y.P., Mash, H., Hadad, C.M., 2009. Photochemical fate of sulfadimethoxine in aquaculture waters. Environ. Sci. Technol. 43, 8587–8592.

Han, S.-K., Bilski, P., Karriker, B., Sik, R.H., Chignell, C.F., 2008. Oxidation of flame retardant tetrabromobisphenol A by singlet oxygen. Environ. Sci. Technol. 42, 166–172.

Hu, L., Flanders, P.M., Miller, P.L., Strathmann, T.J., 2007. Oxidation of sulfamethoxazole and related antimicrobial agents by TiO_2 photocatalysis. Water Res. 41, 2612–2626.

Jeong, J., Song, W., Cooper, W.J., Jung, J., Greaves, J., 2010. Degradation of tetracycline antibiotics: Mechanisms and kinetic studies for advanced oxidation/reduction processes. Chemosphere 78, 533–540.

Jiao, S.J., Zheng, S.R., YIn, D.Q., Wang, L.H., Chen, L.Y., 2008. Aqueous oxytetracycline degradation and the toxicity change of degradation compounds in photoirradiation process. J. Environ. Sci. 20, 806–813.

Jung, J., Kim, Y., Kim, J., Jeong, D.-H., 2008. Environmental levels of ultraviolet light potentiate the toxicity of sulfonamide antibiotics in Daphnia magna. Ecotoxicology 17, 37–45.

Keen, O.S., Linden, K.G., 2013. Degradation of antibiotic activity during UV/H_2O_2 advanced oxidation and photolysis in wastewater effluent. Environ. Sci. Technol. 47, 13020–13030.

Kolpin, D.W., Furlong, E.T., Meyer, M.T., Thurman, E.M., Zaugg, S.D., Barber, L.B., Buxton, H.T., 2002. Pharmaceuticals, hormones, and other organic wastewater contaminants in US streams, 1999-2000: A national reconnaissance. Environ. Sci. Technol. 36, 1202–1211.

Larson, R.A., Weber, E.J., 1996. Reaction mechanisms in environmental organic chemistry. Carbohyd. Polym. 29, 293–294.

Latch, D.E., Stender, B.L., Packer, J.L., Arnold, W.A., McNeill, K., 2003. Photochemical fate of pharmaceuticals in the environment: Cimetidine and ranitidine. Environ. Sci. Technol. 37, 3342–3350.

Leifer, A., 1988. The Kinetics of Environmental Aquatic Photochemistry: Theory and Practice. American Chemical Society: Washington, DC.

Li, K., Zhang, P., Ge, L.K., Ren, H.L., Yu, C.Y., Chen, X.Y., Zhao, Y.F., 2014. Concentration-dependent photodegradation kinetics and hydroxyl-radical oxidation of phenicol antibiotics. Chemosphere 111, 278–282.

Li, Y., Liu, X., Zhang, B., Zhao, Q., Ning, P., Tian, S., 2018. Aquatic photochemistry of sulfamethazine: Multivariate effects of main water constituents and mechanisms. Environ. Sci.: Processes Impacts 20, 513–522.

Li, Y., Qiao, X., Zhang, Y.N., Zhou, C., Xie, H., Chen, J., 2016. Effects of halide ions on photodegradation of sulfonamide antibiotics: Formation of halogenated intermediates. Water Res. 102, 405–412.

Li, Y., Wei, X., Chen, J., Xie, H., Zhang, Y.N., 2015. Photodegradation mechanism of sulfonamides with excited triplet state dissolved organic matter: A case of sulfadiazine with 4-carboxybenzophenone as a proxy. J. Hazard. Mater. 290, 9–15.

Loos, R., Gawlik, B.M., Locoro, G., Rimaviciute, E., Contini, S., Bidoglio, G., 2009. EU-wide survey of polar organic persistent pollutants in European river waters. Environ. Pollut. 157, 561–568.

Luo, Y., Xu, L.Q., Rysz, M., Wang, Y., Zhang, H., Alvarez, P.J.J., 2011. Occurrence and transport of tetracycline, sulfonamide, quinolone, and macrolide antibiotics in the Haihe River Basin, China. Environ. Sci. Technol. 45, 1827–1833.

Managaki, S., Murata, A., Takada, H., Tuyen, B.C., Chiem, N.H., 2007. Distribution of macrolides, sulfonamides, and trimethoprim in tropical waters: Ubiquitous occurrence of veterinary antibiotics in the Mekong Delta. Environ. Sci. Technol. 41, 8004–8010.

Mill, T., 1999. Predicting photoreaction rates in surface waters. Chemosphere. 38, 1379–1390.

Niu, J., Zhang, L., Li, Y., Zhao, J., Lv, S., Xiao, K., 2013a. Effects of environmental factors on sulfamethoxazole photodegradation under simulated sunlight irradiation: kinetics and mechanism. J. Environ. Sci. 25, 1098–1106.

Niu, J.F., Li, Y., Wang, W.L., 2013b. Light-source-dependent role of nitrate and humic acid in tetracycline photolysis: kinetics and mechanism. Chemosphere 92, 1423–1429.

Niu, X.Z., Glady-Croué, J., Croue, J.P., 2017. Photodegradation of sulfathiazole under simulated sunlight: Kinetics, photo-induced structural rearrangement, and antimicrobial activities of photoproducts. Water Res. 124, 576–583.

Oliveros, E., Suardi-Murasecco, P., Aminian-Saghafi, T., Braun, A.M., Hansen, H.J., 1991. 1*H*□Phenalen□1□one: Photophysical properties and singlet□oxygen production. Helv. Chim. Acta 74, 79–90.

Sági, G., Csay, T., Szabó, L., Pátzay, G., Csonka, E., Takács, E., Wojnárovits, L., 2015.

Analytical approaches to the OH radical induced degradation of sulfonamide antibiotics in dilute aqueous solutions. J. Pharmaceut. Biomed. 106, 52–60.

Santoke, H., Song, W., Cooper, W.J., Greaves, J., Miller, G.E., 2009. Free-radical-induced oxidative and reductive degradation of fluoroquinolone pharmaceuticals: Kinetic studies and degradation mechanism. J. Phys. Chem. A 113, 7846–7851.

Schmidt, R., Tanielian, C., Dunsbach, R., Wolff, C., 1994. Phenalenone, a universal reference compound for the determination of quantum yields of singlet oxygen O_2 ($^1\Delta_g$) sensitization. J. Phys. Chem. A 79, 11–17.

Shah, S., Hao, C., 2017. Quantum chemical investigation on photodegradation mechanisms of sulfamethoxypyridazine with dissolved inorganic matter and hydroxyl radical. J. Environ. Sci. 57, 85–92.

Shah, S., Zhang, H., Song, X., Hao, C., 2015. Quantum chemical study of the photolysis mechanisms of sulfachloropyridazine and the influence of selected divalent metal ions. Chemosphere 138, 765–769.

Tentscher, P.R., Eustis, S.N., McNeill, K., Arey, J.S., 2013. Aqueous oxidation of sulfonamide antibiotics: Aromatic nucleophilic substitution of an aniline radical cation. Chem.-Eur. J. 19, 11216–11223.

Trovó, A.G., Nogueira, R.F.P., Agüera, A., Fernandez-Alba, A.R., Sirtori, C., Malato, S., 2009a. Degradation of sulfamethoxazole in water by solar photo-Fenton. Chemical and toxicological evaluation. Water Res. 43, 3922–3931.

Trovó, A.G., Nogueira, R.F.P., Agüera, A., Sirtori, C., 2009b. Photodegradation of sulfamethoxazole in various aqueous media: Persistence, toxicity and photoproducts assessment. Chemosphere 77, 1292–1298.

Vione, D., Minella, M., Maurino, V., Minero, C., 2014. Indirect photochemistry in sunlit surface waters: Photoinduced production of reactive transient species. Chem.-Eur. J. 20, 10590–10606.

Wei, X.X., Chen, J.W., Xie, Q., Zhang, S.Y., Ge, L.K., Qiao, X.L., 2013. Distinct photolytic mechanisms and products for different dissociation species of ciprofloxacin. Environ. Sci. Technol. 47, 4284–4290.

Wei, X.X., Chen, J.W., Xie, Q., Zhang, S.Y., Li, Y.J., Zhang, Y.F., Xie, H.B., 2015. Photochemical behavior of antibiotics impacted by complexation effects of concomitant metals: A case for ciprofloxacin and Cu(II). Environ. Sci.: Processes Impacts 17, 1220–1227.

Werner, J.J., Arnold, W.A., McNeill, K., 2006. Water hardness as a photochemical parameter:

Tetracycline photolysis as a function of calcium concentration, magnesium concentration, and pH. Environ. Sci. Technol. 40, 7236–7241.

Willach, S., Lutze, H.V., Eckey, K., Löppenberg, K., Lueling, M., Wolbert, J.B., Kujawinski, D.M., Jochmann, M.A., Karst, U., Schmidt, T.C., 2018. Direct photolysis of sulfamethoxazole using various irradiation sources and wavelength ranges-insights from degradation product analysis and compound-specific stable isotope analysis. Environ. Sci. Technol. 52, 1225–1233.

Xie, Q., Chen, J.W., Zhao, H.X., Qiao, X.L., Cai, X.Y., Li, X.H., 2013. Different photolysis kinetics and photooxidation reactivities of neutral and anionic hydroxylated polybrominated diphenyl ethers. Chemosphere 90, 188–194.

Xu, J., Hao, Z., Guo, C., Zhang, Y., He, Y., Meng, W., 2014. Photodegradation of sulfapyridine under simulated sunlight irradiation: Kinetics, mechanism and toxicity evolvement. Chemosphere 99, 186–191.

Yang, H., Li, G., An, T., Gao, Y., Fu, J., 2010. Photocatalytic degradation kinetics and mechanism of environmental pharmaceuticals in aqueous suspension of TiO_2: A case of sulfa drugs. Catal. Today 153, 200–207.

Yao, H., Sun, P., Minakata, D., Crittenden, J.C., Huang, C.H., 2013. Kinetics and modeling of degradation of ionophore antibiotics by UV and UV/H_2O_2. Environ. Sci. Technol. 47, 4581–4589.

Zhang, D.N., Yan, S.W., Song, W.H., 2014. Photochemically induced formation of reactive oxygen species (ROS) from effluent organic matter. Environ. Sci. Technol. 48, 12645–12653.

Zhang, Q.Q., Ying, G.G., Pan, C.G., Liu, Y.S., Zhao, J.L., 2015. Comprehensive evaluation of antibiotics emission and fate in the river basins of China: Source analysis, multimedia modeling, and linkage to bacterial resistance. Environ. Sci. Technol. 49, 6772–6782.

Table 1. Expected environmental half-lives ($t_{1/2,E}$, h) for reactions with either •OH or $^1O_2$, and direct photodegradation of sulfonamides (SAs) in sunlit surface waters.

SAs	•OH oxidation[a]		$^1O_2$ oxidation[a]		direct photolysis[b]	
	seawater, pH 7.9–8.4	fresh water, pH 6.0–9.0	seawater, pH 7.9–8.4	fresh water, pH 6.0–9.0	summer, pH 7	winter, pH 7
SMX	29.28–29.29	29.15–29.29	1.01–1.02	1.01–1.77	22	231
SIX	35.33–35.34	34.44–35.34	0.27	0.23–0.27	12	121
SMT	32.84–32.88	29.86–32.89	1.19	1.19–1.54	19	201
ST	14.95–15.85	14.62–27.92	0.82–0.84	0.81–1.01	3	31
SMZ	22.85–25.72	21.17–32.12	0.08–0.13	0.06–1.06	31	180
SM	25.30– 25.75	25.13–31.95	0.34–0.36	0.33–1.19	55	300
SD	24.44– 24.50	24.42–26.47	0.41–0.42	0.41–0.77	31	160
SCP	39.11–39.20	33.88–39.23	0.21	0.08–0.21	9	48
SDM	30.17–30.19	29.33–30.20	1.23–1.25	1.23–2.22	45	420

[a] Calculated based on the •OH and $^1O_2$ concentration levels in the euphotic zone of some surface waters, i.e., [•OH] = 1×10^{-15} M and [$^1O_2$] = 1×10^{-12} M (Cooper et al., 1989; Mill, 1999). [b] Corresponding to direct photolytic half-lives of SAs in near surface waters in midsummer and midwinter at 45° latitude (Boreen et al., 2004, 2005). The half-lives were calculated with quantum yields (correcting for lens effect) and noon-averaged tabulated solar intensities (assuming continuous irradiation) (Leifer, 1988).

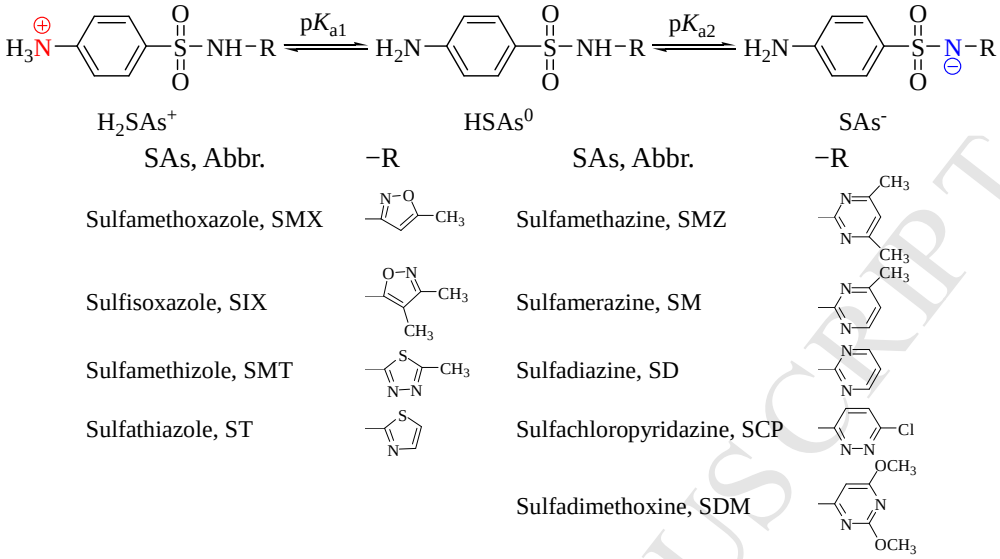

Fig. 1. Chemical structures and the different protonation states of sulfonamide antibiotics (SAs), where H_2SAs^+, $HSAs^0$, and SAs^- represent the cationic form, the neutral form, and the anionic form, respectively.

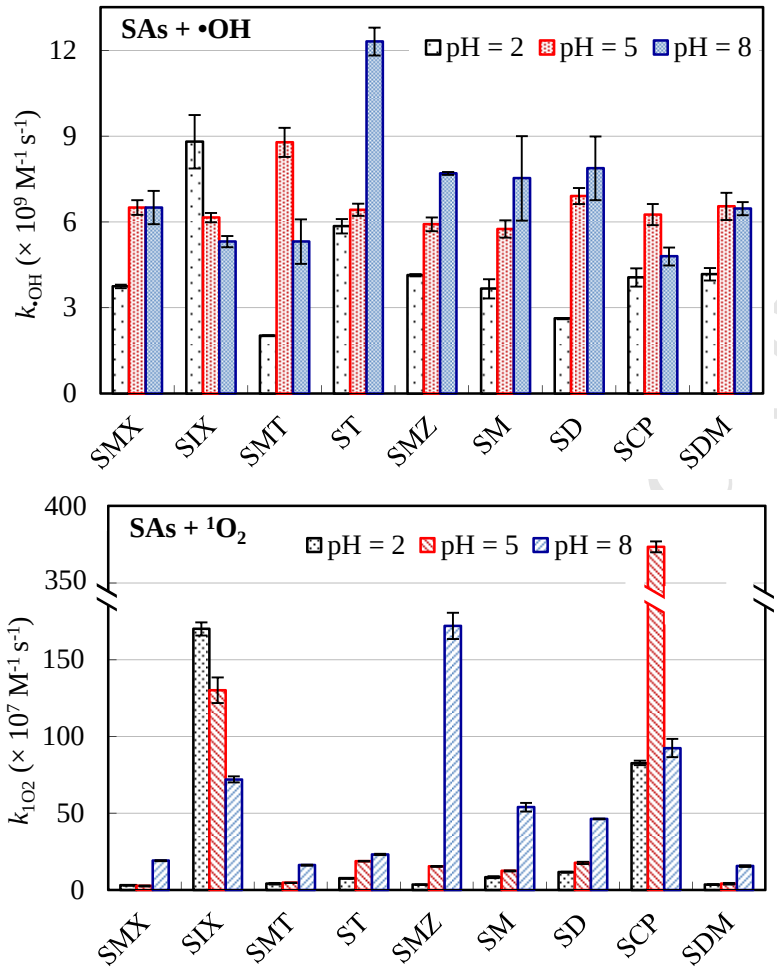

Fig. 2. ROS oxidation rate constants ($k_{\bullet OH}$ and k_{1O2}) of 9 sulfonamide antibiotics (SAs) under different pH conditions

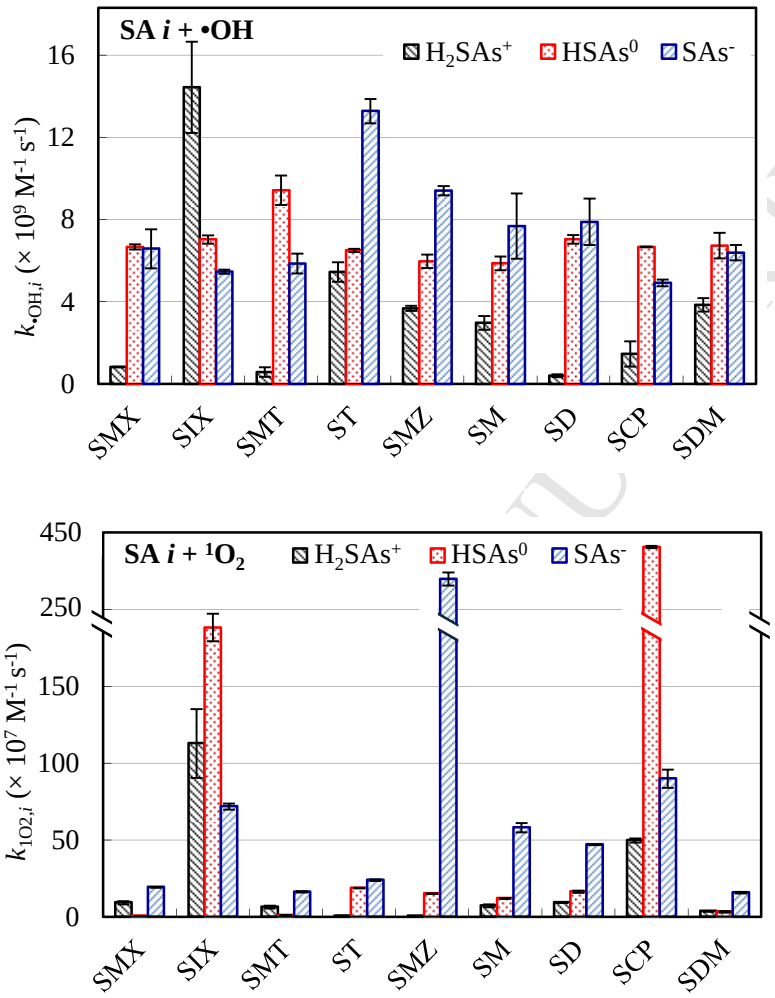

Fig. 3. Bimolecular rate constants ($k_{\bullet OH,i}$ and $k_{1O2,i}$) for the reaction between dissociated SA species (SA *i*) species and ROS

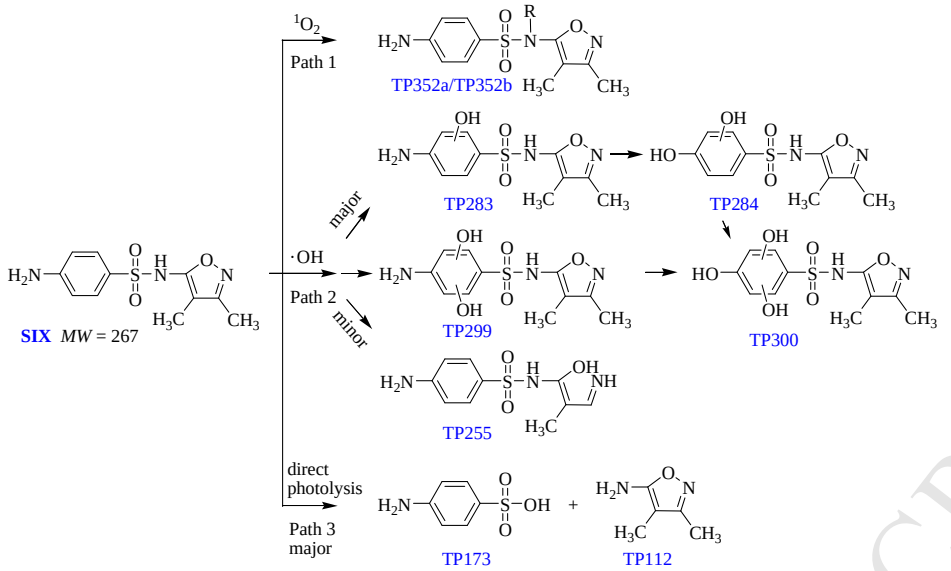

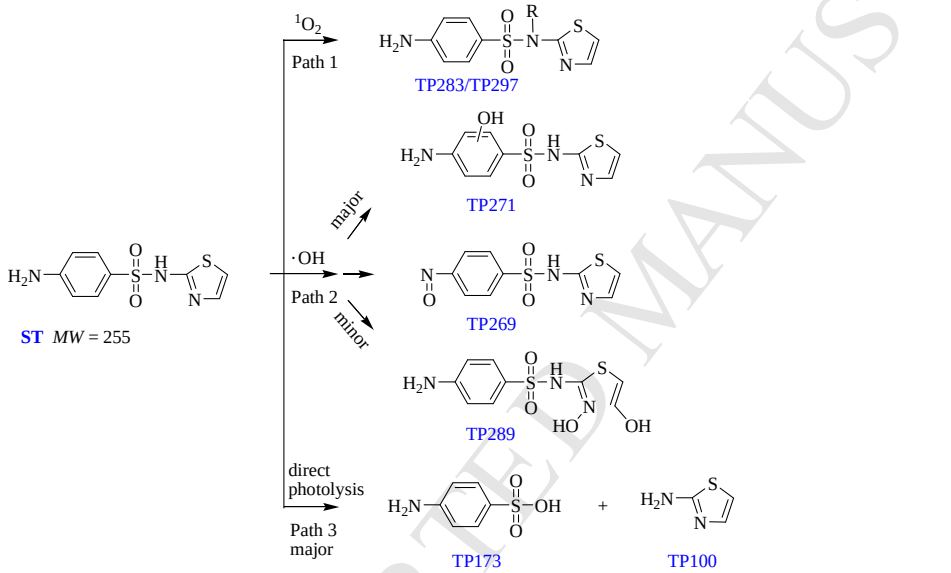

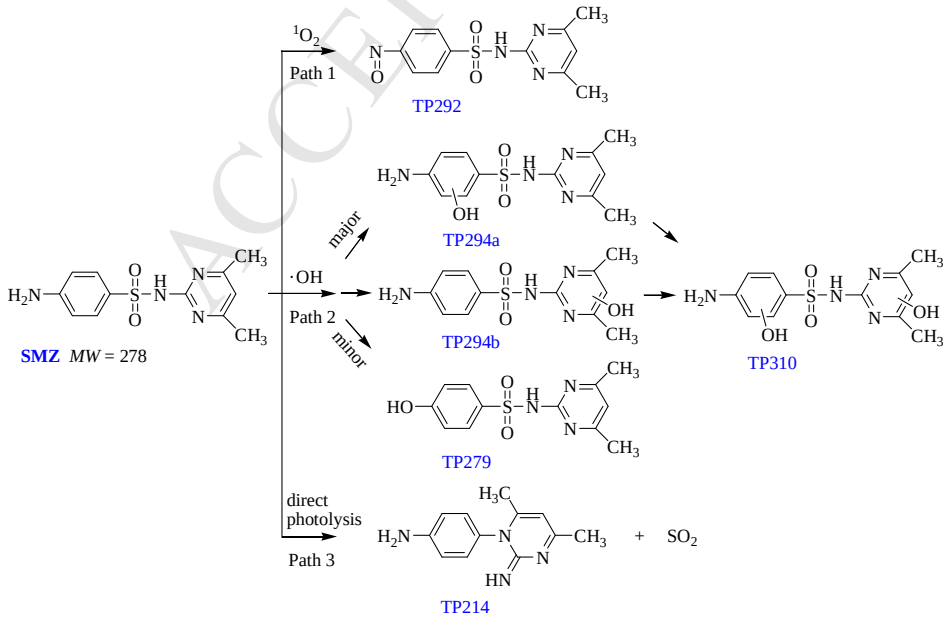

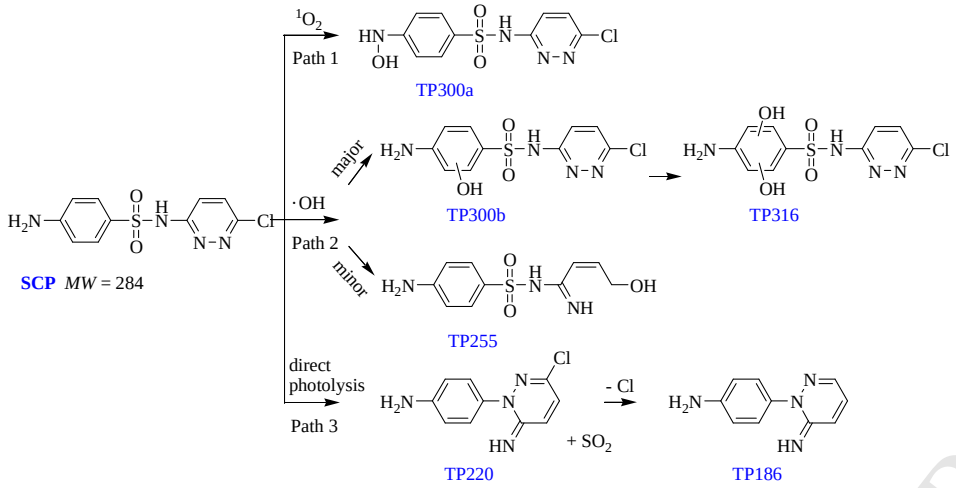

Fig. 4. Proposed phototransformation pathways of four sulfonamide antibiotics, sulfisoxazole (SIX), sulfathiazole (ST), sulfamethazine (SMZ), sulfachloropyridazine (SCP). The transformation products are labeled "TP*n*", with *n* standing for the molecular weight. Pathways of direct photolysis are referred to the previous study (Boreen et al., 2004, 2005).

- Aquatic photooxidation of sulfonamides (SAs) via reactive oxygen species is important
- The kinetics depend on pH and separate reactivities of H_2SAs^+, $HSAs^0$ and SAs^-
- $^1O_2$ plays a key role in aquatic fate of SAs compared with •OH and direct photolysis
- Different primary pathways and multiple intermediates occur for the three reactions